Quantification of lead melting in a radioactive transport cask using CFD

Priyanshu Goyal*, Vishnu Verma, Anu Dutta, J. Chattopadhyay
Reactor Safety Division
Bhabha Atomic Research Centre, Trombay, Mumbai-400085, India

ABSTRACT

Shielded shipping casks are commonly used for the transportation of radioactive waste materials. Design approval of such a cask by the regulatory authority is subject to its demonstration of compliance with a thermal test, also known as fire test (among other tests). Lead shielding usually is provided for radiation protection. During cask transportation, an accident may cause fire, which may result in melting of lead provided for cask shielding. The molten lead may come out in case of mechanical seal failure resulting in shielding loss. Hence, cask has to maintain its structural integrity under normal and accidental (fire) conditions, and needs to be qualified with the prescribed code guidelines by the regulatory authorities. The present work reports a comprehensive CFD analysis of the thermal behaviour of lead melting for two different geometries (cylindrical and rectangular) considering natural convection in the melt. The study reveals a substantial influence of natural convection on the thermal state and melting behaviour of lead which may have a great bearing on the safety during transportation of cask.

Keywords: CFD, fire test, melting, natural convection, transport cask

Introduction

A typical radioactive material transportation cask consists of a rectangular shaped box made of stainless-steel with an inner cavity to store the radioactive material for transportation. The inner cavity is encapsulated by lead sandwiched between two stainless steel liners. The lead provides the necessary shielding to minimize the radiation dose to the public domain. Design approval of such casks by the regulatory authority [1] is subject to its demonstration of compliance with a fire test (among other tests), which consists of exposure of the cask to hydrocarbon fuel/air fire on all sides with a flame temperature of about 800°C for a period of 30 minutes. During the fire test, the radiative flux from the fire is incident on the outer surface of the cask, which causes rapid heating of the various inner elements of the cask, and may cause melting of the shielding material i.e., lead. The melting of lead can cause loss of shielding capability due to relocation of molten lead in the lower region of the cask, thus creating space in the top region. The molten lead may come out in case of mechanical seal failure due to high temperature and radiation dose may leak into the public domain. Therefore, it is of utmost importance to calculate the amount of lead melted during the fire test so as to assess the possible loss of shielding. The confirmation of design compliance mentioned above is generally shown by carrying out detailed steady-state and transient thermal analysis of the cask, which involves solving the basic transient 3-D conduction equation (ignoring natural convection) with the appropriate radiative and convective boundary conditions [2]. However, ignoring the natural (buoyancy driven) convection because of the density gradients in the molten pool of the lead may lead to a significant error in the predictions of both the extent of melting of lead and the pattern of melt front propagation during the transients. Not much literature is available on thermal analysis of transportation casks involving natural convection in the molten pool. This is due to the fact that numerical simulation of convective flow and heat transfer in the presence of phase change is a challenging task because the heat transfer is coupled with the turbulent flow field in 3D in a global domain where the pure solid and the pure liquid phases are separated by an ever-changing interface. At RSD, BARC, CFD analysis has been carried out for several transportation casks for the demonstration of their compliance with regulatory guidelines. The present article briefly describes the CFD analysis and the effect of natural convection phenomenon on thermal analysis of two different representative transportation casks.

Geometries of selected shipping casks and test conditions

Two casks with different shape and size – one with a rectangular cross-section and the other with a cylindrical cross-section have been considered in the present analysis. Fig. 1 depicts the cross-section of the two casks.

Considering the symmetry axes in the rectangular and cylindrical cask, only sections of the entire cask were analyzed. For the rectangular cask, 3D analysis was done for the 1/4th section of the cask, retaining full vertical height to simulate the natural convection, which is a function of height. For the cylindrical cask, the axis is considered the symmetry axis. For the cylindrical cask, 2D axisymmetric case was analyzed.

Under normal storage conditions, the entire heat generated within the cask gets dissipated to the surroundings from its outer surface by natural convection and radiation mechanisms. Under

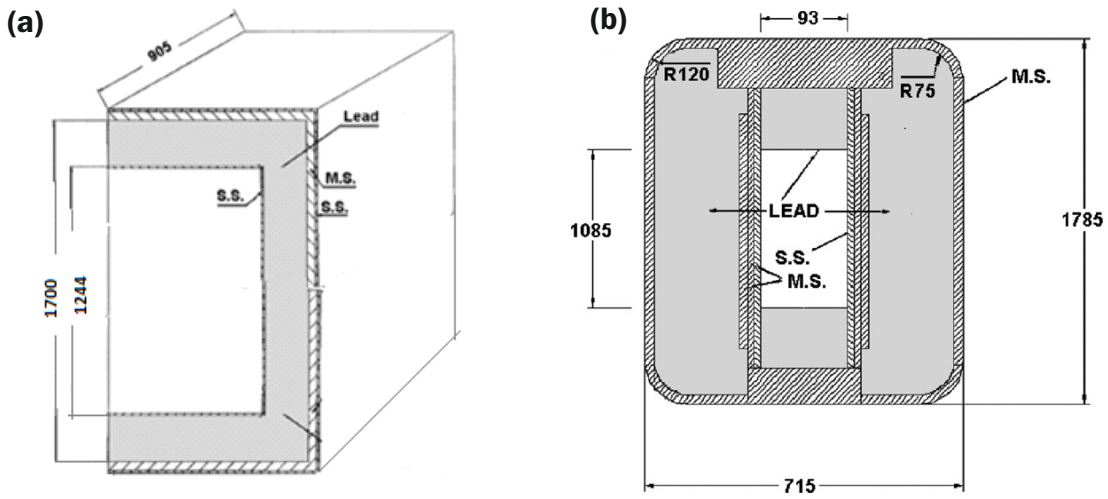

Fig.1: Sectional view of transportation cask (a) 1/4th section of rectangular cask (b) 1/2 section of cylindrical cask

the specified ambient conditions, the cask outer surface also receives solar radiation, which is dissipated to the surroundings. There is a possibility of melting of the lead layer in the annular region of the transport cask during an accidental fire. The regulatory guidelines stipulate that the fire test is to be carried out after the cask attains the steady-state in normal storage conditions. After the fire test, the analysis is continued with normal ambient conditions till the time temperature starts reducing in the cask. With this objective, the analysis was performed in three stages:

- Steady-state analysis
- Fire test analysis
- Post fire analysis

During transportation, the cask will be exposed to solar insolation and the values for the same are taken as per regulatory guidelines [1]. The heat generated within the over pack is specified as surface heat flux on the inner surface of the cask (for a typical case, heat generation of 456 W is taken for cylindrical cask and 7.4 kW for the rectangular cask). The heat generation is more in rectangular cask because of its larger Curie content compared to cylindrical cask. The emissivity of outer steel surface is taken as 0.3. The ambient temperature is specified as 42 °C. Convective heat transfer coefficient of 5W/m^{2}K has been specified on the outer surface of the cask.

The steady state temperature distribution so obtained is used as initial temperature distribution for analyzing the transients during the fire test. During the fire test of 30 min duration, the radiative heat flux from the fire is incident on the outer walls, which will cause rapid heating of the various inner elements of the cask. Internal heat generation due to radioactive decay is same as in case of normal conditions. Ambient temperature of 800 °C, surface absorptivity of 0.8 and flame emissivity of 1.0 are specified for fire test condition. No solar heat flux is considered on the outer surface. Convective heat transfer coefficient on the outer surface typically recommended is 15 W/m^{2}K which is based on a flue gas velocity of 10 m/s [1]. The temperature dependent thermophysical properties of various materials, such as, lead, mild steel (MS) and stainless steel (SS) are taken from literature [3].

Numerical Modeling

The thermal analysis of cylindrical transport cask was carried out at RSD, BARC [4] using commercially available CFD code CFD-ACE+ [5], while the analysis of rectangular cask was carried out by Sanyal et al. at CGCRI, Kolkata (using CFD code FLUENT) under BRNS project with RSD [6]. At the time when the job was taken up, FLUENT already was capable of handling lead melting phenomenon through its inbuilt module. However, CFD-ACE+, at that time, had no inbuilt module to handle melting/solidification phenomenon directly. Therefore, with the help of user-subroutines, CFD-ACE+ was modified to model melting/solidification phenomenon.

The numerical model of the thermal transport in the cask and turbulent momentum transport of molten lead in the cask has been developed as a closely coupled set of transport equations for mass, energy and momentum along with turbulent fields, such as, turbulent kinetic energy and dissipation rate, using enthalpy porosity technique [7]. The set of governing equations in terms of primitive variables are as follows:

Continuity:

$$\frac{\partial \rho}{\partial t} + \nabla \cdot (\rho \vec{V}) = 0 \quad (1)$$

Momentum transport:

$$\frac{\partial \rho u}{\partial t} + \nabla \cdot (\rho \vec{V} u) = \nabla \cdot (\mu \nabla u) - \frac{\partial P}{\partial x} - \mathrm{A}u + \tau_{turb} \quad (2)$$

$$\frac{\partial \rho v}{\partial t} + \nabla \cdot (\rho \vec{V} v) = \nabla \cdot (\mu \nabla v) - \frac{\partial P}{\partial y} - \mathrm{A}v + \rho_{\mathrm{ref}} g \beta \left(\frac{h - h_{\mathrm{ref}}}{C_{\mathrm{p}}}\right) + \tau_{turb} \quad (3)$$

$$\frac{\partial \rho w}{\partial t} + \nabla \cdot (\rho \vec{V} w) = \nabla \cdot (\mu \nabla w) - \frac{\partial P}{\partial x} - \mathrm{A}w + \tau_{turb} \quad (4)$$

u, v, w are the velocity components in x, y and z directions, respectively. $\vec{V}$ is the velocity vector, P is pressure, μ is the viscosity , ρ is the density, β is thermal expansion coefficient and h_{ref} and ρ_{ref} are reference values of enthalpy and density, respectively. C_p is specific heat capacity and τ_{turb} represents Reynolds stress due to turbulence[5].

Since buoyancy-driven natural convection generates a very high Rayleigh number flow (Ra 10^{10}-10^{12}) in the molten lead during fire test, it is imperative to consider an appropriate turbulence model and couple the turbulence transport equations with the continuity, momentum and energy conservation equations. As reported by Sanyal *et al.* [6] based on the experimental studies of Ozoe *et al.* [8], Choi *et al.*[9], Michalek [10], k-ω shear stress transport (SST) model of turbulence is the best suited for simulating moderate to high Rayleigh number natural convection-driven turbulent flow of fluids with or without phase change. Therefore, for the analyses of both the casks, k-ω SST model of turbulence, developed by Menter [11], has been adopted. The model blends the k-ω formulation in the near-wall region with a modified k-ε formulation in the far field employing a suitable blending function.

Turbulent transport:

The governing equations of the turbulence model are given below.

$$\frac{\partial(\rho k)}{\partial t} + \nabla \cdot \left(\rho \vec{V} k\right) = \nabla \cdot (\Gamma_k \nabla k) + G_k - Y_k + S_k \quad (5)$$

$$\frac{\partial(\rho \omega)}{\partial t} + \nabla \cdot \left(\rho \vec{V} \omega\right) = \nabla \cdot (\Gamma_\omega \nabla \omega) + G_\omega - Y_\omega + S_\omega + D_\omega \quad (6)$$

where Γ_i $(i=k,\omega)$ is the effective diffusivity, G_i $(i=k,\omega)$ represents the generation, Y_i $(i=k,\omega)$ represents the dissipation and S_i $(i=k,\omega)$ represents the source term for k and ω,respectively. In Eq. (6), D_ω represents a cross-diffusion term for ω. The detailed definition of these terms are available in Menter [11] and are not presented here for the sake of brevity.

Energy transport:

The energy transport equation is given below.

$$\frac{\partial \rho h}{\partial t} + \nabla \cdot \left(\rho \vec{V} h\right) = \nabla \cdot (\eta \nabla h) - \frac{\partial \rho \Delta H}{\partial t} - \nabla \cdot \left(\rho \vec{V} \Delta H\right) \quad (7)$$

$h = \int_{T_{ref}}^{T} c_p dT$ is the sensible enthalpy, η ($\eta = k/\rho c_p$)is thermal diffusivity, and ΔH is the latent heat content and is a function of temperature.

The latent heat content can also be written in terms of the latent heat of the material (L) as given by Eq. (8).

$$\Delta H = \mathrm{sL} \quad (8)$$

where s is the liquid fraction and can be defined for the temperature between solidus and liquidus temperature as:

$$\mathrm{s} = \frac{T - T_{solidus}}{T_{liquidus} - T_{solidus}} \text{ with } T_{solidus} < \mathrm{T} < T_{liquidus} \quad (9)$$

Liquid fraction for the temperature in liquidus and solidus region can be given as

$$\mathrm{s} = 0 \quad \text{if} \quad T < T_{solidus}$$

$$\mathrm{s} = 1 \quad \text{if} \quad T > T_{liquidus}$$

The condition that all velocities in solid regions are zero is accounted for in the enthalpy-porosity approach by appropriately defining the parameter A in equations (2),(3) and (4). The basic principle is to gradually reduce the velocities from a finite value in the liquid to zero in the full solid. In order to achieve this behaviour, an appropriate definition of A is given as [7]:

$$\mathrm{A} = -\lambda \frac{(1-s)^2}{s^3 + b} \quad (10)$$

where b is a small computational number (0.00001) to avoid division by zero and λ is a very large number (10^9) [12].

It should be mentioned that although any convenient model may be acceptable for extinguishing velocities in solidifying cells in isothermal phase change systems, it is desirable that the method chosen allows a smooth, gradual transition rather than a step-change in the velocity. Step changes in the momentum equation source term tend to retard numerical convergence and may even lead to divergence.

The following assumptions were made during the analysis:

- Considering geometrical and thermal symmetry, a 2D axisymmetric model of the cylindrical cask and a 3D model representing 1/4th part of the rectangular cask were considered.
- For simplifying the CFD model and reducing the computational effort, the fuel bundles, trays, lifting arrangements and supports were not modeled.
- The internal heat generation in the spent fuel was applied in terms of average heat flux on the inner surface of the cask.
- Differential expansion and Marangoni convection of molten lead during fire and post fire test condition were not considered.

The following boundary conditions for heat transport are applied under normal, fire test and post-fire cool-down conditions:

Normal:

$$-k_{ss} \frac{\partial T_{co}}{\partial n} = h_{co,\infty}\left(T_{co,s} - T_\infty\right) + \sigma \varepsilon_s \left(T_{co,s}^4 - T_\infty^4\right) - \alpha_{co,s} q_{co,solar} \quad (11)$$

Fire Test:

$$-k_{ss} \frac{\partial T_{co}}{\partial n} = h_{co,f}\left(T_f - T_{co,s}\right) + \sigma \epsilon_f T_f^4 - \sigma \epsilon_{co,s} T_{fco,s}^4 \quad (12)$$

Post-Fire Cool Down:

$$-k_{ss} \frac{\partial T_{co}}{\partial n} = h_{co,pf}\left(T_{co,s} - T_\infty\right) + \sigma \varepsilon_s \left(T_{co,s}^4 - T_\infty^4\right) \quad (13)$$

n is the local normal to the surface, σ is the Stefan–Boltzmann's constant, ε is the emissivity and α is the absorptivity. Subscripts *ss, co, f, pf* and *s* refer to stainless steel, cask outer, fire, post fire and surface, respectively.

Solution Methodology

For comparison purpose, two sets of simulations were carried out for transient fire analysis. In one simulation, analysis was carried out considering only pure conduction, and in the second simulation, the effect of natural convection with phase change along with full turbulent coupling was considered. Pressure–velocity coupling was achieved using SIMPLE algorithm of Patankar[13]. At first, the steady-state solution was achieved. The thermal state of the cask obtained as the steady-state solution was considered as the initial condition for the transient fire test for 30 min. Iterative implicit algorithm was employed for solving transient flow. The analyses revealed a significant change in the melting pattern with full convective and

turbulent coupling compared to the results obtained for conductive melting alone.

The 2-D axisymmetric simulation (with approximately 30,000 cells) of cylindrical cask was carried out on Quad-core CPU machine. The steady-state analysis took one-hour machine time to complete. The pure conduction fire-test analysis of 1800 s took 80 hours of machine time while the fire-test analysis with natural convection consideration took 300 hours of machine time. The 3-D simulation of rectangular cask (with approximately 3.5 lakh cells) was carried out on eight-core XEON machine. The steady-state analysis took two-hour machine time to complete. The pure conduction fire-test analysis of 1800 s took 300 hours of machine time while the fire-test analysis with natural convection consideration took 1300 hours of machine time.

Results and Discussions

At first, steady state temperature profiles were computed for the cylindrical and rectangular casks considering internal heat generation due to radiation from the inner bundle, solar insolation on the outer surface and heat dissipation due to convective heat transfer from the outer walls to the ambient. The temperature profiles for the casks of different cross-sections are depicted in Fig. 2. From this figure, it can be observed that under steady-state conditions, the maximum computed temperature in the cylindrical cask is 352 K, and the minimum computed temperature is 343.8 K. The maximum temperature occurs at the top half of the inner surface. The temperature falls from the inner to the outer wall in the cask. Since the maximum temperature is much lower than the melting point of lead, thermal transport occurs through pure conduction across the solid steel shells and shielding lead. The curved thermal contours are typical of conductive thermal profile with a thermal source in the inner wall. Similarly, for the rectangular cask, the maximum steady-state temperature is 392 K, and the minimum temperature is 368 K. Again, in this case, thermal transport occurs by means of pure conduction only.

The temperature distribution obtained as a solution of the steady state analysis is used as the initial condition for the subsequent transient analysis under fire test conditions with natural convection. For the cylindrical cask, the transient case was run with adaptive time-stepping for maximum time step of 0.1 s and a minimum time step of 10^{-5} s, respectively up to a time of

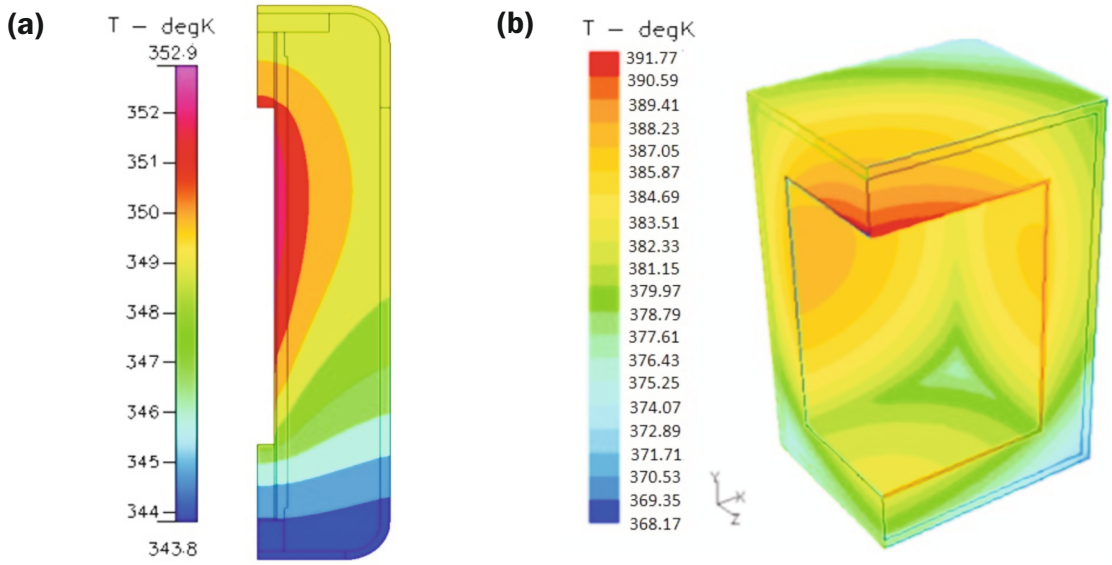

Fig.2: Steady state temperature profiles in (a) cylindrical cask (b) rectangular cask (1/4th section)

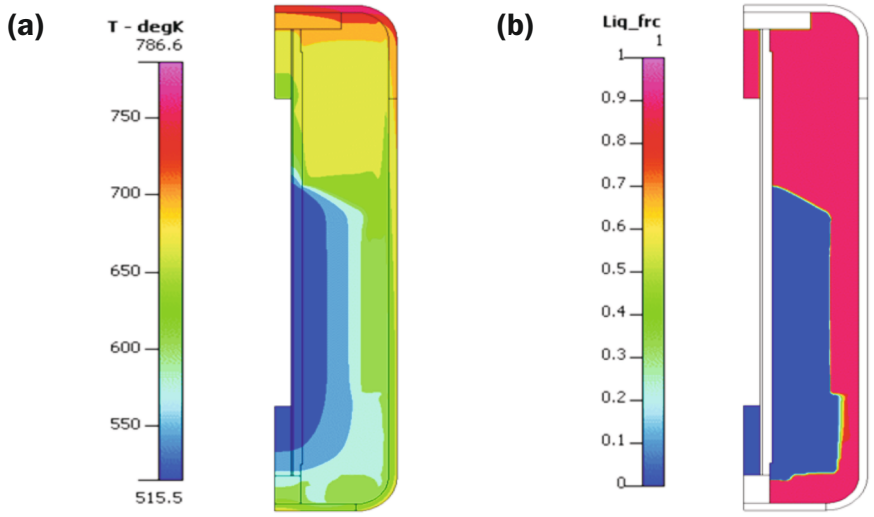

Fig.3: (a)Temperature contours and (b) melt interface contours at the end of fire test simulation for cylindrical transport cask considering natural convection

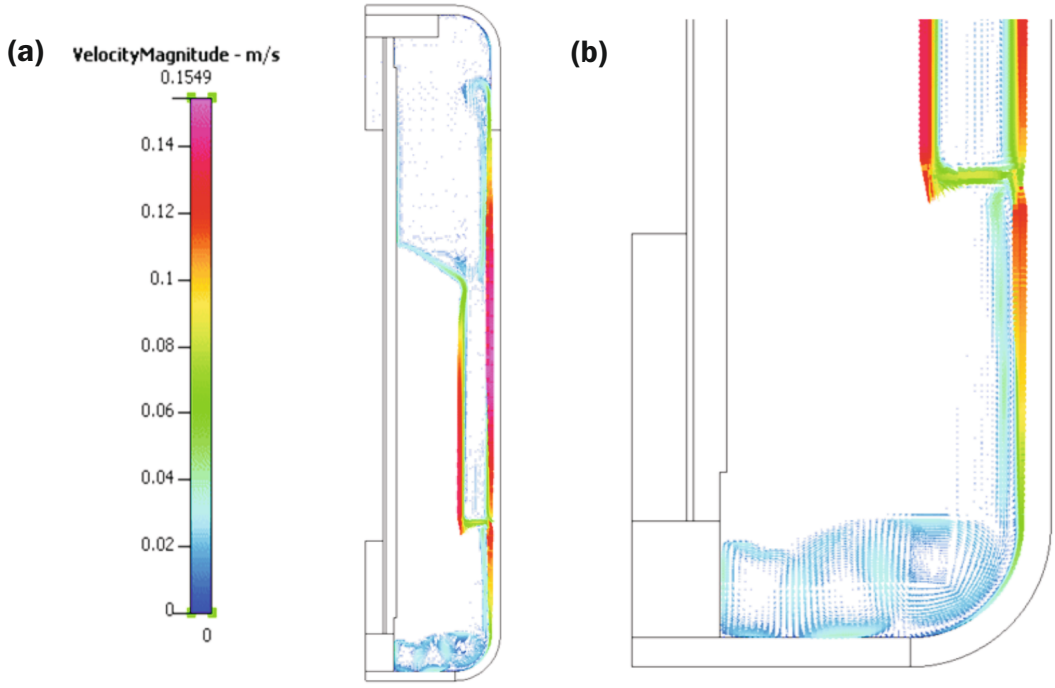

Fig.4: Velocity vectors (a) full view and (b) bottom zone view at the end of fire test simulation for cylindrical transport cask considering natural convection

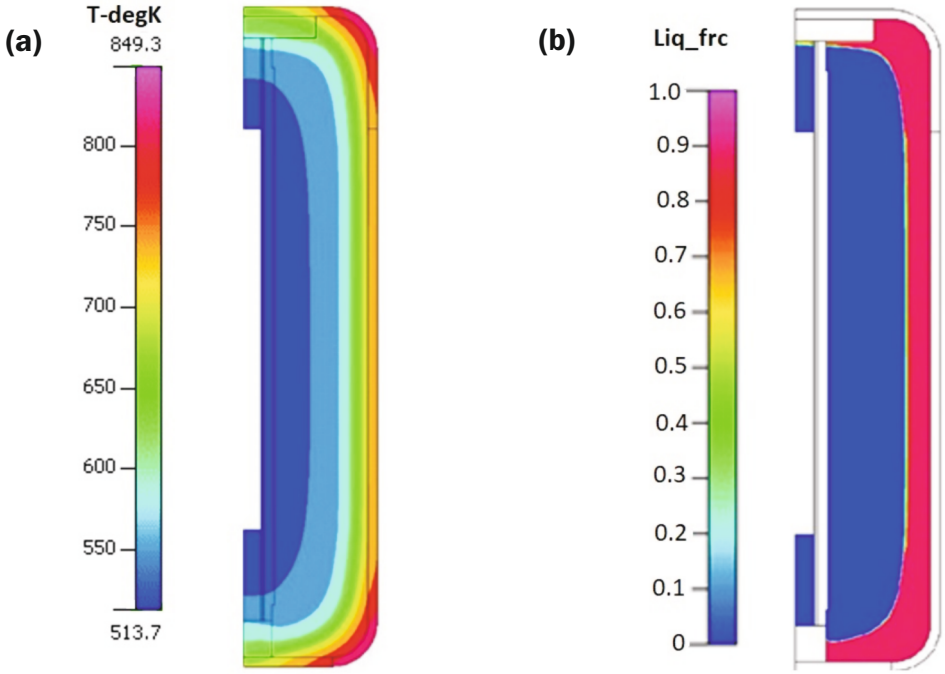

Fig.5: (a)Temperature contours and (b) melt interface contours at the end of fire test for cylindrical transport cask considering pure conduction

1800s. The thermal contours and lead melt interface at t = 1800s for the cylindrical cask are shown in Fig. 3, while the velocity vectors are shown in Fig. 4.

From Figs. 3 and 4, it can be observed that thermal profiles are dictated by the high Rayleigh number convection patterns in the cask. There is a dominant anti-clockwise recirculation loop across the vertical direction of the cask with vertically downward flow along the melt interface and vertically upward flow along the cask wall. At the bottom of the cask, the flow exhibits multiple counteracting recirculation loops. This is typical of Rayleigh Bernard instability which originates at the bottom of cask due to a relatively thin layer of molten lead trapped between the bottom wall of the cask and the solid lead. The Rayleigh Bernard flow with counteracting loops sets in because the molten lead at this location experiences higher temperature at the bottom wall and lower temperature at the melt interface.

For the sake of comparison, the temperature contours and melt front of cylindrical cask for pure conduction are presented in Fig.5. Conductive heat transport results in thermal and phase change contours symmetric with respect to the horizontal axis, which is physically inaccurate due to the effect of buoyancy being neglected. Fig. 6 depicts the comparison between the computed thermal profiles for convective and conductive melting of lead in the cylindrical cask obtained along the horizontal and vertical

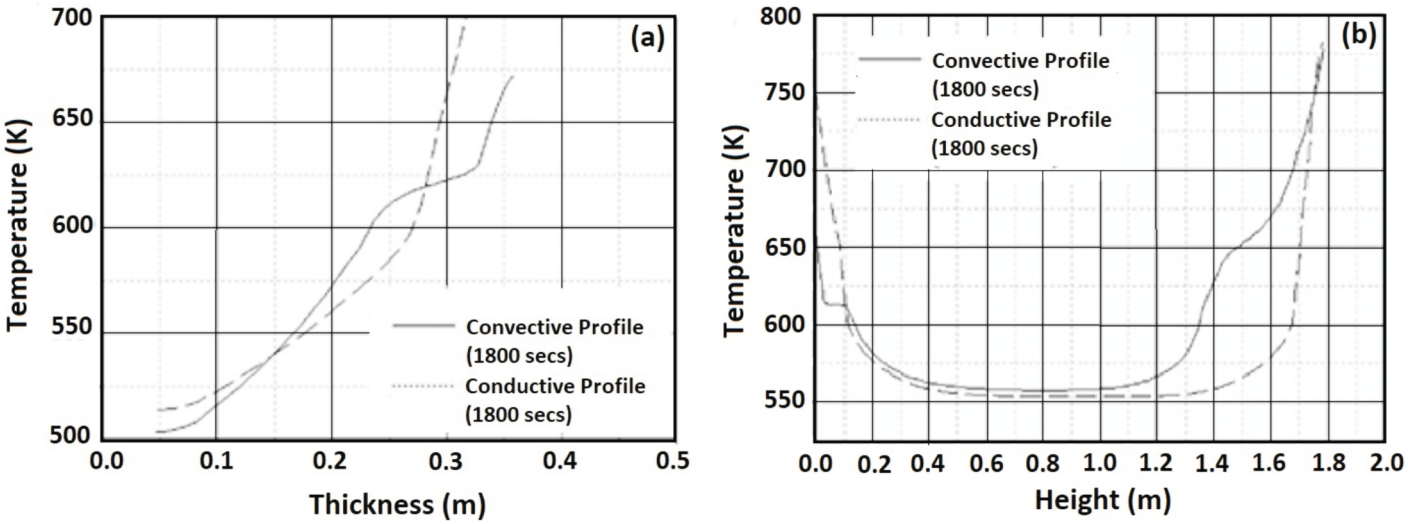

Fig.6: Comparison between temperature profiles in cylindrical cask (a) along the thickness at mid height and (b) along the height at mid thickness

direction at mid height and mid thickness of the cavity, respectively, at the end of the fire test.

From Figs. 5 and 6, it is observed that the profiles obtained for high Rayleigh number convection is significantly different from the profiles obtained computationally using the assumption of pure conductive heat transport in the cask. Along the thickness, the convection creates steep thermal gradient across the inner and outer walls of the cask than that in case of the conductive melting. Near the core, convection creates a nearly constant temperature unlike that for pure conduction. Along the height, convective heat transport results in an asymmetric thermal profile with respect to the horizontal axis unlike the nearly perfect symmetric thermal profile obtained using pure conduction analysis.

As a consequence of the effects of natural convection, the nature and extent of lead-melting in the cylindrical cask under convective flow is substantially different from that of conductive melting. At the end of 30 min of fire test, the lead melting for pure conduction analysis is 33% (v/v), while the extent of lead-melting estimated under convective melting is as high as 70% (v/v), which is more than twice the figure estimated by conductive melting. Moreover, the shape of the solid-liquid interface is substantially different in convective melting compared to the case of conductive melting due to high Rayleigh number turbulent convection.

From the analysis of the cylindrical cask, it was established that ignoring natural convection during thermal analysis of cask leads to erroneous results. Hence, the computations for rectangular cask were only carried out by considering natural convection. The $k-\omega$ SST model with appropriate wall functions was employed with variable time stepping of maximum time step of 0.1 s and a minimum time step of 10^{-5} s, up to 1800s. Figs. 7 and 8 show the temperature contours and melt interface contours for the rectangular cask, respectively.

In Fig. 8, it is clearly shown that after 30 minutes, melting of lead takes place only at a small fraction of the cavity volume at the top and bottom corners of the cavity. The rectangular cask is substantially larger than the cylindrical cask, resulting in much-reduced melting,11% (v/v), at the end of the fire test, compared to more than six-fold melting in the case of the cylindrical cask.

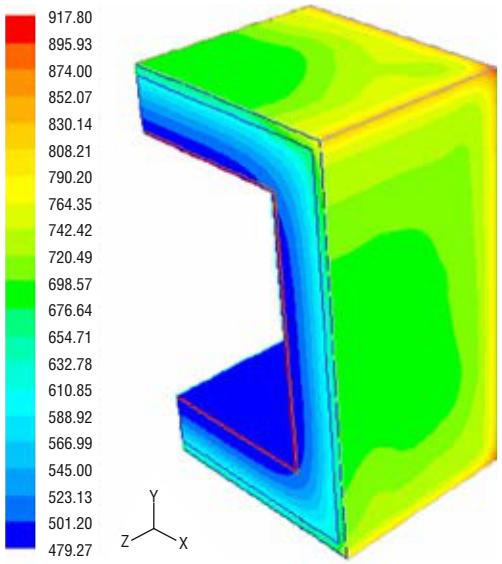

Fig.7: Temperature Contours in the rectangular cask (1/4th section) due to convective melting of lead at the end of fire test at 1800s (Full View)[6]

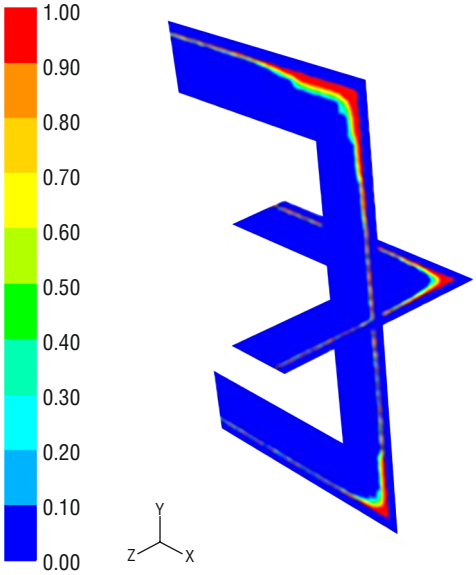

Fig.8: Melt interface contours in the rectangular cask (1/4th section) due to convective melting of lead at the end of fire test at 1800s across mid-planes perpendicular to Y and Z-axes[6]

For both the casks, since the melting patterns do not change in post-fire conditions, those results are not presented here for the sake of brevity.

Conclusions

Comprehensive CFD analysis of transportation cask for two different geometries (cylindrical and rectangular) have been carried out considering natural convection in the lead melting. The study reveals a substantial influence of natural convection on the thermal state and melting behaviour of lead which may have a great bearing on the safety during transportation of cask. It was found that Rayleigh number convection was pronounced on the extent of melting of the lead layer in comparison with the conductive melting simulation study. Convective melting led to 70% (v/v) melting of lead layer in the cylindrical cask at the end of the fire test, compared to 33% (v/v) melting estimated in the case of conductive heat transport alone. For the larger cask of rectangular cross-section, the amount of melting was substantially smaller (approx. 11% by volume) compared to that of the cylindrical cask. The present work shows that the thermal design of a transport cask based only on conductive melting is grossly inaccurate and needs close coupling with an accurate turbulence model to account for the effects of high Rayleigh number convection generated during the fire test in a cask.

Corresponding author*

Priyanshu Goyal (pgoyal@barc.gov.on)

References

[1] Code for Safety in Transport of Radioactive Materials, AERB Code No. SC/TR-1, 1986.

[2] C.F. Bonilla, A.L. Strupczewski, *Nuclear Structural Engineering*,1965, **2**, 40.

[3] Eric. A. Brandes, Smithells Metals Handbook, Fulmer Research Institute Ltd, 6th Edition.

[4] Chikanna Gowda, Priyanshu Goyal "Thermal Analysis of Transport Cask for Natural Convection During Melting of Lead: CFD Simulation", M. Tech Thesis, June, 2009.

[5] CFD-ACE+ User manuals, ESI CFD IncV2009.

[6] D. Sanyal, A. Chakraborty, V. Verma, P. Goyal, Final Report, BRNS Project, CSIR-CGCRI, Kolkata, India, 2005/36/7-BRNS/2283.

[7] A.D. Brent, V.R. Voller and K.J. Reid, *Numerical Heat Transfer*,1988,**13**, 297.

[8] Ozoe, H., Mouri, A., M. Ohmuro, *Int. J. Heat Mass Transfer*, 1985, **28**, 125.

[9] S.K. Choi, E.K. Kim, S.O. Kim, *5th Asian Computational Fluid Dynamics*, Busan, Korea, 2003, 27.

[10] T. Michalek, *Numerical Heat Transfer*, Gliwice-Cracow, Poland, 2005.

[11] F.R. Menter, *AIAA J.*,1994, **32**,1598.

[12] R. Viswanath and Y. Jaluria, *Numerical Heat Transfer Part B - Fundamentals*, 1993, **24**, 77.

[13] S.V. Patankar, *Numerical Heat Transfer and Fluid Flow*,1980.